Plasmonic nanodome array fabricated on plastic as a dual-mode surface plasmon resonance and surface-enhanced Raman scattering sensor

C. Choi and S. Semancik

National Institute of Standards and Technology, Gaithersburg, MD, USA, charles.choi@nist.gov

ABSTRACT

Label-free optical sensors have recently emerged as a highly sensitive approach for detecting a broad range of chemical and biological analytes that include illicit drug compounds, explosives, proteins, viruses, and bacteria.To best meet such diverse monitoring needs, different sensing methods have been used. For example, detection of chemical compounds typically requires specific chemical identification method, such as Raman spectroscopy, while proteins or bacteria are most effectively detected by performing capture affinity assays using surface plasmon resonance biosensors. Therefore, the integration of multiple detection modalities into a single, substrate-based sensing platform would offer highly complementary capabilities that allow a variety of analytes to be detected simultaneously. This work describes a label-free, optical sensor system fabricated on a flexible plastic film using nanoreplica molding process with dual detection modalities: surface-enhanced Raman scattering (SERS) for specific chemical identification and localized surface plasmon resonance (LSPR) for capture affinity biosensing. The sensor surface is comprised of a close-packed array of 383 nm diameter dome structures with interdome spacing of 14 nm, fabricated by a process that combines nanoreplica molding and unpatterned blanket deposition of SiO_2 and Ag thin films.

Keywords: label-free optical sensor, nanodome, surface plasmon resonance, surface-enhanced Raman scattering, replica molding

1 INTRODUCTION

Label-free optical biosensors have recently emerged as a highly sensitive approach for detecting a broad range of biological analytes that include proteins, DNA/RNA, viruses, bacteria, and cells [1-5]. Biosensors based on plasmonic nanostructures, in particular, have been extensively studied due to their unique optical properties that are capable of supporting localized surface plasmon resonance (LSPR). LSPR is a phenomenon associated with free electrons of a material collectively oscillating in resonance, driven by an incident electromagnetic field (light), leading to significant enhancement of the electromagnetic field with a high degree of spatial confinement around the nanostructure, well below the dimensions of the optical diffraction limit. The subwavelength confinement of the enhanced optical mode produced by LSPR offers excellent sensitivity to the local interfacial environment. Since biomolecular interactions occur on, or very near, the surface of the sensor structure, the highly confined and enhanced optical modes produced by LSPR can be employed as a means for highly sensitive detection of a broad range of biological analytes with minimal interference from the surrounding bulk media [6, 7].

Due to its capability for specific chemical identification through measurement of vibrational energies associated with chemical bonds in molecules, Raman spectroscopy is a powerful and versatile method for label-free molecular identification. As a general purpose analytical method, the applications for Raman spectroscopy span a broad range of fields that includes protein–protein interaction analysis, DNA/RNA hybridization, aptamer conformational change, viral particle detection, bacteria identification, and detection of explosives [8]. As first observed and theoretically understood, the extremely small Raman scattering cross section may be enhanced when a molecule is in close proximity to a roughened metal surface that supports regions of heightened electromagnetic field intensity [9, 10]. The SERS enhancement achieved via LSPR enables Raman scattering spectra to be gathered rapidly with substantially less laser power, allowing the detection technique to be more feasible, provided that the analytes have an opportunity to come into contact with the SERS-active surface.

This work describes a label-free, optical sensor system fabricated on a flexible plastic film using nanoreplica molding process with dual detection modalities: surface-enhanced Raman scattering (SERS) for specific chemical identification and localized surface plasmon resonance (LSPR) for capture affinity biosensing. The sensor surface is comprised of a close-packed array of 383 nm diameter dome structures with interdome spacing of 14 nm, fabricated by a process that combines nanoreplica molding and unpatterned blanket deposition of SiO_2 and Ag thin films.

2 RESULTS AND DISCUSSION

2.1 Nanodome array

Figure 1 shows the scanning electron microscope (SEM) and images of the completed SERS nanodome array substrates fabricated on flexible PET sheets, cut into 70 × 100 mm^2 area. The nanoreplica molding process was performed over an area of 120 × 120 mm^2.

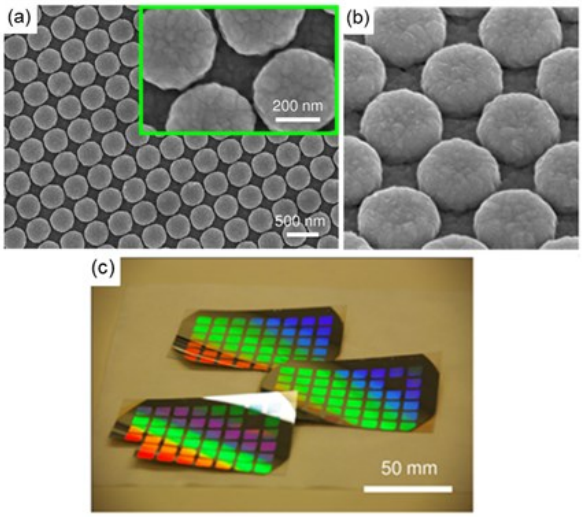

Figure 1: (a)-(b) SEM images of the nanodome array substrate. (c) Image of the completed SERS nanodome array substrates fabricated on flexible plastic sheets, cut into 70 × 100 mm^2 area.

2.2 Localized surface plasmon resonance

Figure 2(a) shows the extinction spectrum, which is experimentally measured from the nanodome array exposed to deionized (DI) water, plotted as a solid blue curve. The measured extinction spectrum matches well with the result obtained from a finite-difference time-domain (FDTD) simulation, which is plotted as a dashed red curve. Figure 2(b)-(d) show the top views and cross-sectional views of 2-D spatial electric field intensity profiles of one unit volume of the nanodome array for the grating diffraction mode at 533 nm, the higher-order multipole mode at 581 nm, and the dipole mode at 926 nm, respectively. The scale bars on the right side represent resonant electric field intensity (E^2) levels normalized with respect to the incident electric field intensity (E_{inc}^2) on a logarithmic scale. In the FDTD model, the incident field was set as a plane wave propagating along the –z direction towards the nanodome surface at normal incidence with polarization (direction of the electric field) set along the x direction.

The sensitivity of the nanodome array to changes in the bulk refractive index (n) was measured by exposing the sensor surface to air (n = 1), DI water (n = 1.333), acetone (n = 1.359) and isopropyl alcohol (n = 1.377) in sequence. Figure 3(a) shows the result of the peak wavelength value (PWV) shift for each resonance mode as a function of refractive indices of the fluid media on the surface of the nanodome sensor. In the plot, dipole, multipole, and grating diffraction modes are represented by blue dots, green triangles, and red hollow circles, respectively, with the error bars (not visible on all data points due to small magnitudes of the deviations) representing ± 1 standard deviation for five different sensing regions within the nanodome sensor area. Bulk refractive index sensitivity (S_b = ΔPWV/Δn) measured for dipole, multipole, and grating diffraction modes were 626 nm, 375 nm, and 345 nm, respectively.

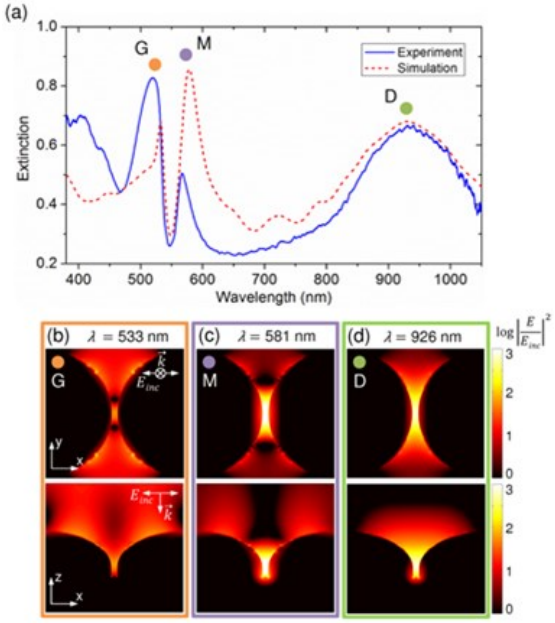

Figure 2: (a) Extinction spectra of the nanodome array. (b) to (d) 2-D spatial distribution of the electric field intensity for the Ag nanodome array for grating diffraction (G), multipole (M), and dipole modes (D). Top-views and cross-sectional views of field intensity distributions for one unit volume of the array are shown.

In bioassay experiments using capture affinity-based sensors, most of the biomolecular binding interactions occur near the surface of the sensor, so the sensitivity near the surface of the sensor provides a more accurate metric of the performance of the biosensor, compared to the bulk sensitivity. The response of the nanodome sensors were measured as a function of distance from the surface using stacked alternating layers of charged polyelectrolyte deposited onto the surface. Figure 3(b) shows the result of the surface sensitivity measurement, displaying the kinetic sensor response of the peak wavelength value (PWV) shift as a function of time for polyethylenimine (PEI) and seven poly(sodium styrene sulfonate) (PSS) - poly(allylamine hydrochloride) (PAH) depositions, with the measurement interval set to 60 sec. Again, the dipole, multipole, and grating diffraction modes are represented by blue dots, green triangles, and red hollow circles, respectively.

In order to demonstrate the utility of the plasmonic nanodome array for detecting biomolecules, a bioassay was performed to measure the binding affinity constant of a protein-protein interaction between protein A and human immunoglobulin G (IgG). For the assay, protein A was adsorbed on the sensor surface by noncovalent hydrophobic attachment, and the modified surface was subsequently

exposed to human IgG antibody under a range of concentrations. Figure 3(c) shows the PWV-shift end point as a function of human IgG concentration for the dipole, multipole, and grating diffraction modes. The PWV-shift end points for each of the modes were fitted with a nonlinear dose-response curve and the dissociation constants (K_D) obtained were 0.693 µmol/L, 0.672 µmol/L, and 0.690 µmol/L for the dipole, multipole, and grating diffraction modes, respectively.

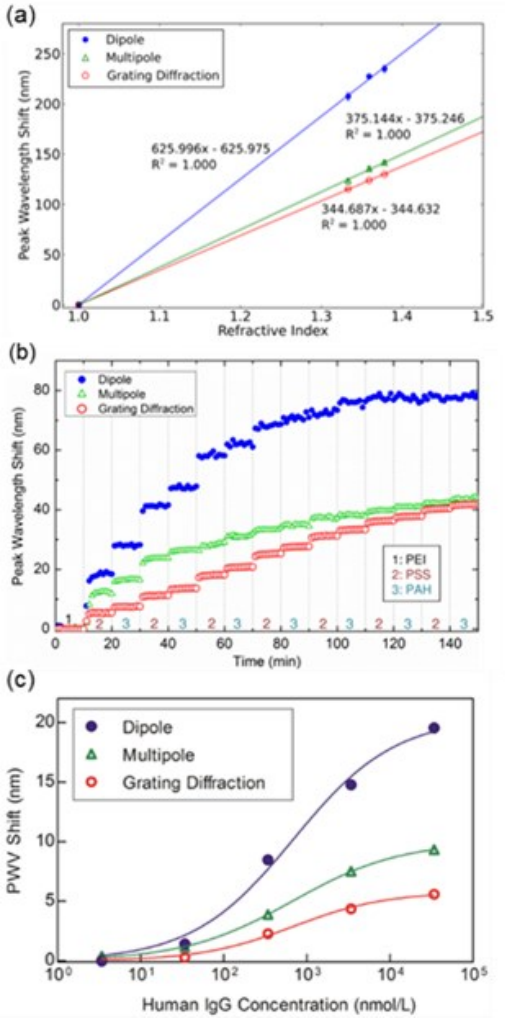

Figure 3: (a) Extinction spectra of the nanodome array. (b) to (d) 2-D spatial distribution of the electric field intensity for the Ag nanodome array for grating diffraction (G), multipole (M), and dipole modes (D). Top-views and cross-sectional views of field intensity distributions for one unit volume of the array are shown.

2.3 Surface-enhanced Raman scattering

In order to experimentally measure the SERS enhancement factor for the nanodome array substrates, a concentration series of R6G molecules (1 nM–10 µM) were deposited on a SERS sensor surface. 1 mM R6G was also deposited on the same substrate in the area outside of the nanodome region to serve as a reference. Figure 4(a) shows the SERS spectra measured.

Fig. 4(b) compares the SERS spectra for promethazine solutions of varying concentrations from 3.13 to 50 mg/mL, the range typically delivered to patients. The SERS spectra of promethazine solution exhibited dominant Raman intensity peaks located at 1030 cm^{-1}, due to the ring-breathing mode of the aromatic rings, and at 1567 cm^{-1} and 1589 cm^{-1}, corresponding to aromatic C-C stretching modes of the molecule. Using the dominant peak located at 1030 cm^{-1} for analysis of promethazine, the inset shows the plot of the average Raman intensity as a function of promethazine concentration with error bars indicating ±1 standard deviation measured from five separate concentration series (N = 5). In each series, a single SERS measurement was made for each analyte concentration, where a wash step consisting of emptying and flowing through 5 mL of buffer solution was repeated three times between each analyte concentration. A linear fit between the Raman intensity at 1030 cm^{-1} and the concentration of promethazine yielded an R^2 value of 0.999. This demonstrates that the nanodome sensor may be used to identify promethazine in solution and the Raman peak magnitude is linearly proportional to its concentration.

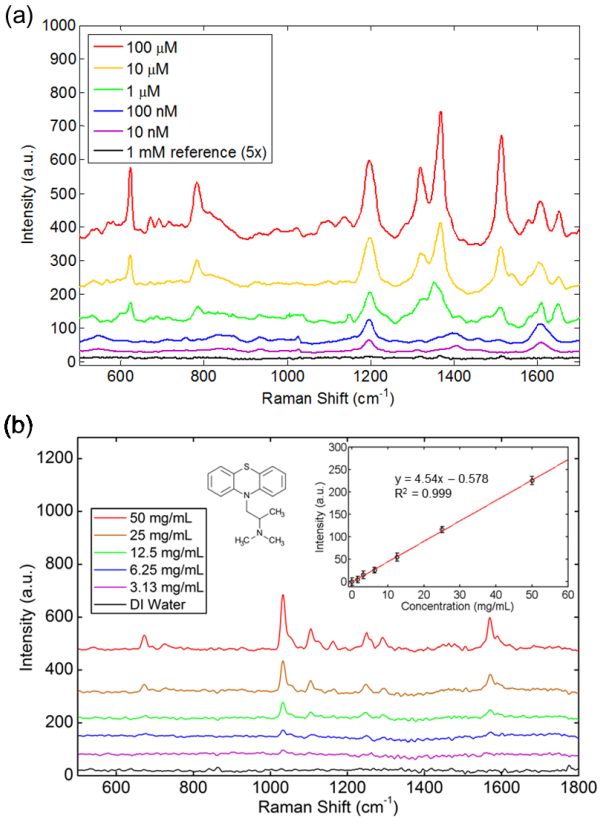

Figure 4: (a) SERS spectra of R6G molecules on the nanodome substrate. (b) SERS spectra for promethazine solution. Inset: Raman intensity measured at 1030 cm^{-1} as a function of promethazine concentration.

3 CONCLUSION

This work describes a label-free photonics-based sensor system fabricated on a flexible plastic film using nanoreplica molding process that is capable of multiple detection modalities: SERS for specific chemical identification and LSPR for capture affinity biosensing. The integration of multiple detection modalities into a substrate-based single sensing platform, as in the system described in this work, is a novel technology offering highly complementary information allowing for wide range of analytes to be detected simultaneously. In addition, a single sensor structure with multiple detection modalities offers an efficient and economical system since the cost associated with fabrication of separate sensor structures and integration/packaging of each sensor types can be avoided.

REFERENCES

[1] J. Homola, S. S. Yee, and G. Gauglitz, "Surface plasmon resonance sensors: review," Sensors and Actuators B-Chemical, vol. 54, pp. 3-15, Jan 25 1999.

[2] A. Brecht and G. Gauglitz, "Optical Probes and Transducers," Biosensors & Bioelectronics, vol. 10, pp. 923-936, 1995.

[3] L. L. Chan, S. L. Gosangari, K. L. Watkin, and B. T. Cunningham, "Label-free imaging of cancer cells using photonic crystal biosensors and application to cytotoxicity screening of a natural compound library," Sensors and Actuators B-Chemical, vol. 132, pp. 418-425, Jun 16 2008.

[4] M. F. Pineda, L. L. Y. Chan, T. Kuhlenschmidt, C. J. Choi, M. Kuhlenschmidt, and B. T. Cunningham, "Rapid Specific and Label-Free Detection of Porcine Rotavirus Using Photonic Crystal Biosensors," Ieee Sensors Journal, vol. 9, pp. 470-477, Apr 2009.

[5] A. D. Taylor, J. Ladd, Q. M. Yu, S. F. Chen, J. Homola, and S. Y. Jiang, "Quantitative and simultaneous detection of four foodborne bacterial pathogens with a multi-channel SPR sensor," Biosensors & Bioelectronics, vol. 22, pp. 752-758, Dec 15 2006.

[6] J. N. Anker, W. P. Hall, O. Lyandres, N. C. Shah, J. Zhao, and R. P. Van Duyne, "Biosensing with plasmonic nanosensors," Nature Materials, vol. 7, pp. 442-453, Jun 2008.

[7] W. J. Galush, S. A. Shelby, M. J. Mulvihill, A. Tao, P. D. Yang, and J. T. Groves, "A Nanocube Plasmonic Sensor for Molecular Binding on Membrane Surfaces," Nano Letters, vol. 9, pp. 2077-2082, May 2009.

[8] K. Hering, D. Cialla, K. Ackermann, T. Dorfer, R. Moller, H. Schneidewind, R. Mattheis, W. Fritzsche, P. Rosch, and J. Popp, "SERS: a versatile tool in chemical and biochemical diagnostics," Analytical and Bioanalytical Chemistry, vol. 390, pp. 113-124, Jan 2008.

[9] Fleischm.M, P. J. Hendra, and Mcquilla.Aj, "Raman-Spectra of Pyridine Adsorbed at a Silver Electrode," Chemical Physics Letters, vol. 26, pp. 163-166, 1974.

[10] D. L. Jeanmaire and R. P. Vanduyne, "Surface Raman Spectroelectrochemistry .1. Heterocyclic, Aromatic, and Aliphatic-Amines Adsorbed on Anodized Silver Electrode," Journal of Electroanalytical Chemistry, vol. 84, pp. 1-20, 1977.